

In_{0.6}Ga_{0.4}As/GaAs quantum-dot infrared photodetector with operating temperature up to 260 K

Lin Jiang and Sheng S. Li

Electrical and Computer Engineering Department, University of Florida, Gainesville, Florida 32611

Nien-Tze Yeh and Jen-Inn Chyi

Electrical Engineering Department, National Central University, Chung-Li, Taiwan, 32054, Republic of China

C. E. Ross and K. S. Jones

Department of Material Science and Engineering, University of Florida, Gainesville, Florida 32611

(Received 30 September 2002; accepted 2 December 2002)

A high-sensitivity In_{0.6}Ga_{0.4}As/GaAs quantum-dot infrared photodetector (QDIP) with detection wave band in 6.7–11.5 μm and operating temperature up to 260 K under normal incident illumination has been demonstrated. The peak detection wavelength shifts from 7.6 to 8.4 μm when the temperature rises from 40 to 260 K. The background limited performance (BLIP) detectivity (D_{BLIP}^*) measured at $V_b = -2.0$ V, $T = 77$ K, and $\lambda_p = 7.6$ μm was found to be 1.1×10^{10} $\text{cm Hz}^{1/2}/\text{W}$, with a corresponding responsivity of 0.22 A/W. The high operating temperature is attributed to the very low dark current and long carrier lifetime in the quantum dots of this device. The results show that this QDIP can operate at high temperature without using the large band gap material such as AlGaAs or InGaP as blocking barrier to reduce the device dark current. © 2003 American Institute of Physics. [DOI: 10.1063/1.1540240]

In the past few years, quantum-dot infrared photodetectors (QDIPs) have emerged as promising devices for long wavelength infrared (LWIR) detection due to their potential advantages over the conventional quantum-well infrared photodetectors (QWIPs). The advantages include: (1) intrinsic sensitivity to normal incident infrared light, (2) longer lifetime of excited electrons due to greatly suppressed electron-phonon scattering, and (3) the predicted significantly lower dark current.¹ These unique properties arise from three-dimensional carrier confinement of quantum dots. Although many earlier experiments showed that the performance of QDIPs was still inferior to QWIPs,^{1–4} However, recently, several groups reported that InAs/GaAs QDIPs could achieve higher operating temperature (>100 K) by using a large band gap material such as AlGaAs or InGaP as the blocking barrier to reduce the device dark current.^{5–7} In this work, we report a high sensitivity In_{0.6}Ga_{0.4}As/GaAs QDIP with operating temperature up to 260 K without using the wide band gap (AlGaAs or InGaP) current blocking barrier.

The sample was grown on a (100) GaAs semi-insulating substrate using the Stranski–Krastanov growth mode by molecular beam epitaxy technique. Before the growth of QDIP structure, a 0.5 μm GaAs buffer layer was grown on the GaAs substrate. The active region consists of ten periods of In_{0.6}Ga_{0.4}As/GaAs quantum dots (QDs), and the GaAs spacer thickness is 600 Å. The complete active region was sandwiched by a 5000 Å *n*-type GaAs top contact layer and a 1 μm bottom contact layer. These contact layers were doped with Si to 2.0×10^{18} cm^{-3} . The nominal thickness for the In_{0.6}Ga_{0.4}As QDs is 5 monolayer (ML), and the QDs are Si doped to 8.0×10^{17} cm^{-3} . The In_{0.6}Ga_{0.4}As QD growth rate was 0.5 ML/s, and the GaAs spacer growth rate is 1 $\mu\text{m}/\text{h}$.

The growth temperature was 580 °C for the GaAs buffer and contact layers, and 520 °C for the In_{0.6}Ga_{0.4}As QDs and GaAs spacers. The atomic force microscopy images revealed that the average QD density is 1.2×10^{10} cm^{-2} , and the average size of the QDs is 26 nm in diameter and 6 nm in height. Figures 1(a) and 1(b) show two photos of the cross-section transmission electron microscopy of the QDIP structure.

Mesa structures with an active area of 200×200 μm^2 were created by using standard photolithography and wet chemical etching. A square ohmic contact ring composed of AuGe/Ag/Au films was deposited on the periphery of the highly doped contact layers of the mesa structure and alloyed for ohmic contacts. The role of Ag film is to block Au from permeating the device. The low melting point and excellent conductivity of Ag makes it easy to grow the low-resistance ohmic contact.

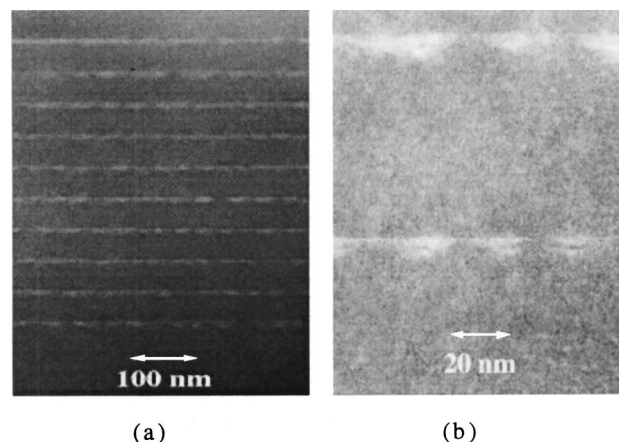


FIG. 1. Cross-section transmission electron microscopy photos: (a) 100 nm scale and (b) 20 nm scale for the In_{0.6}Ga_{0.4}As/GaAs QDIP.

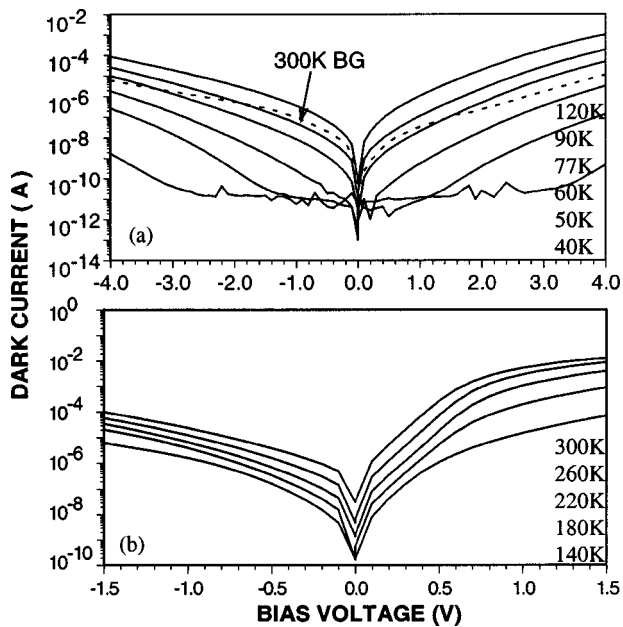


FIG. 2. Dark current density vs bias voltage for the InGaAs/GaAs QDIP: (a) for $40\text{ K} \leq T \leq 120\text{ K}$ and (b) $140\text{ K} \leq T \leq 300\text{ K}$.

Realizing that the reported spacer widths for QDIPs with AlGaAs or InGaP current blocking barrier were less than 50 nm,⁵⁻⁷ we used a thicker spacer (60 nm) of GaAs instead of a large band gap material to reduce the device dark currents, which consist of thermal exciting current, thermally assisted tunneling current, and tunneling current. By using a thicker spacer one could reduce the tunneling current and thermally assisted tunneling current components in the dark currents without blocking the photocurrent in the conduction band of QDIP. Figure 2 shows the temperature-dependent dark I - V curves along with the 300 K-background window current with a 180° field of view. In Fig. 2(a), the dark current was measured at $T=40, 50, 60, 77, 90,$ and 120 K with V_b varying from -4.0 to 4.0 V . The dark current ($I_D=8.3 \times 10^{-9}\text{ A}$, $V_b=-1\text{ V}$, $T=77\text{ K}$) is much lower than that measured in a similar InGaAs/GaAs QDIP with a 30 nm GaAs spacer and QDs doped to $6 \times 10^{17}\text{ cm}^{-3}$ ($I_D=1.1 \times 10^{-5}\text{ A}$, $V_b=-1\text{ V}$, $T=70\text{ K}$).³ The background limited performance (BLIP) condition was obtained at $-2.2\text{ V} < V_b < 0\text{ V}$ and 90 K and at $0\text{ V} < V_b < 1.6\text{ V}$ and 77 K . The slightly asymmetrical dark I - V characteristic is due mainly to the asymmetry of dot shape. Figure 2(b) shows the dark current measured at temperatures of 140, 180, 220, 260, and 300 K and $-1.5 < V_b < 1.5\text{ V}$. At $T=260\text{ K}$ and $V_b=-0.5\text{ V}$, the dark current is $1.5 \times 10^{-6}\text{ A}$ ($J_D=3.75 \times 10^{-3}\text{ A/cm}^2$) which is still comparable to the dark current of a normal LWIR InGaAs/GaAs QWIP at $T=90\text{ K}$ ($J_D=4 \times 10^{-3}\text{ A/cm}^2$, $V_b=-1\text{ V}$).⁸ At lower temperatures [Fig. 2(a)], the rapid increase of dark current with temperature is due mainly to its exponential dependence on temperature. However, at higher temperatures [Fig. 2(b)], the rate of increase is greatly reduced, which is attributed to the saturation of thermally excited electrons in the QDs by the limited average sheet electron density of the device.⁹ The asymmetry of the dark I - V curves shown in Fig. 2(b) is caused by the asymmetrical carrier injection from the bottom and top contact layers in different current directions under high tempera-

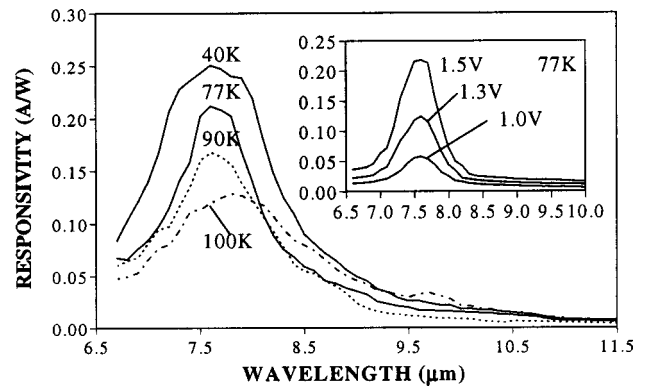


FIG. 3. Responsivity vs wavelength measured at $T=40\text{ K}$ ($V_b=-2.3\text{ V}$), 77 K (-2.0 V), 90 K (-1.9 V), and 100 K (-1.8 V).

tures. With the depletion of electrons from QDs, the electrons from contact layer become a dominant factor to influence the dark current. Under positive bias, more electrons are injected from the bottom contact layer to the top contact layer because of the higher sheet electron density of the bottom contact layer, thus the dark current under negative bias is lower than the positive bias condition.

The photocurrent spectra were measured under normal incident illumination using a 0.25 m grating monochromator and calibrated blackbody source at $T=1000^\circ\text{C}$. The photocurrent signal of the device was measured using a low-noise operational amplifier and a DSP locking amplifier.

Figure 3 shows the spectral responsivities measured at $T=40\text{ K}$ ($V_b=-2.3\text{ V}$), 77 K (-2.0 V), 90 K (-1.9 V), 100 K (-1.8 V), and the bias voltages were chosen to obtain the highest signal to noise ratio in the corresponding temperatures. At $V_b=-2.3\text{ V}$ and $T=40\text{ K}$, a peak responsivity of 0.25 A/W was obtained at $\lambda_p=7.6\text{ }\mu\text{m}$. The cuton and cutoff wavelengths for the full width at half maximum are 7.0 and $8.3\text{ }\mu\text{m}$, with $\Delta\lambda/\lambda_p=17.1\%$. The peak wavelength is at $7.6\text{ }\mu\text{m}$ when the temperature is below 100 K , and a slight redshift occurs when the temperature increases above 100 K , and a second peak at $9.7\text{ }\mu\text{m}$ appears meanwhile. The redshift of peak detection wavelength is due to the energy change of QD ground state with increasing temperature.¹⁰ In addition, when the temperature is increased, the Fermi distribution function was broadening, and more electrons occupied in the higher energy states. When these electrons were photoexcited from QDs, the second absorption peak could be observed. The inset shows the spectral responsivities measured below 77 K and at different biases of $V_b=1.5, 1.3,$ and 1.0 V . The peak wavelength was found independent of bias voltage at fixed temperatures.

Due to the low dark current, the spectral response of this QDIP was observed up to a temperature as high as 260 K before the dark current exceeding the photocurrent (i.e., $S/N < 1$). Figure 4 shows the responsivity versus wavelength measured at $T=160\text{ K}$ ($V_b=-0.80\text{ V}$), 180 K (-0.71 V), 200 K (-0.68 V), 220 K (-0.62 V), 240 K (-0.59 V), and 260 K (-0.55 V). The bias voltages were chosen to achieve maximum photocurrent to dark current ratio. As shown, the maximum responsivity obtained at 160 K and $V_b=-0.80\text{ V}$ was 0.11 A/W at $\lambda_p=8.1\text{ }\mu\text{m}$, and the second peak responsivity was 27 mA/W at $9.7\text{ }\mu\text{m}$. At 260 K and $V_b=-0.55\text{ V}$, the peak responsivity was 6.1 mA/W at λ_p

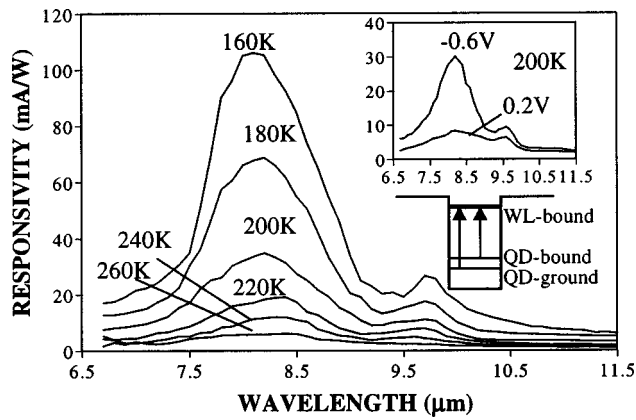


FIG. 4. Responsivity vs wavelength measured at $T=160$ K (-0.80 V), 180 K (-0.71 V), 200 K (-0.68 V), 220 K (-0.62 V), 240 K (-0.59 V), and 260 K (-0.55 V).

$=8.4 \mu\text{m}$. The $\Delta\lambda/\lambda_p$ (λ_p is the first peak) value varies from 14.3% to 14.8%. We found both the responsivity and bias voltage decreased with increasing temperature under maximum photocurrent to dark current ratio, which was consistent with the dark $I-V$ characteristics shown in Fig. 2. The inset in Fig. 4 shows the responsivity versus wavelength measured at $T=200$ K and $V_b=-0.6$ and 0.2 V.

The narrow absorption band of the device indicates that the optical transition is due to the bound-to-bound states intersubband transition. Since the size and shape of the dots which affect the electronic levels¹⁰ cannot be accurately determined, and the strain tensor of the dots is complicated, it is difficult to obtain the true band structure of the device. Several groups have performed theoretical calculations of QD systems to account for the observed intersublevel energies.^{11–13} According to the calculated estimation for a typical InGaAs/GaAs QDs (i.e., 15–28 nm in base width, 3–7 nm in height), the energy difference from the ground bound state of QDs to the wetting-layer bound state was around 100–300 meV, the energy separation between the electron states in QDs was from 30 to 80 meV.^{12,13} The photon absorption peaks (163–127 meV) and the energy separation of the electron states in QDs (~ 36 meV) that we observed were in reasonably good agreement with the estimation, and we believed that the absorption was due to the QD first and second bound states to wetting-layer bound states as shown in Fig. 4. It is noted that, besides the low dark current, another key factor for the mechanism of high temperature operation is the intrinsic property of zero-dimensional device: the large electron relaxation time from the excited states to the ground state in quantum dots, which

makes photoexcited electrons difficult to be recaptured by QDs, can increase the signal to noise ratio and allow for high operating temperature.^{7,14}

The peak BLIP detectivity can be expressed as¹⁵

$$D_{\text{BLIP}}^* = \frac{\lambda}{2hc} \left(\frac{\eta g}{Q_b} \right)^{1/2}, \quad (1)$$

where η is the net quantum efficiency, λ is the wavelength, h is the Planck constant, c is the speed of light, Q_b is the photon flux of the incident background blackbody radiation, and ηg can be calculated from the measured responsivity. At $V_b=-2.0$ V and $T=77$ K, D_{BLIP}^* was found to be 1.1×10^{10} $\text{cm Hz}^{1/2}/\text{W}$ at $\lambda_p=7.6 \mu\text{m}$.

In conclusion, we have demonstrated a high sensitivity In_{0.6}Ga_{0.4}As/GaAs QDIP with spectral response falls in the 6.7–11.5 μm wave band and operating temperature up to 260 K. The normal incident responsivity was obtained from $T=40$ K up to $T=260$ K. The BLIP detectivity at $V_b=-2.0$ V and $T=77$ K was 1.1×10^{10} $\text{cm Hz}^{1/2}/\text{W}$ at $\lambda_p=7.6 \mu\text{m}$. The results reveal that this QDIP device can be operated at a temperature as high as 260 K with reducing dark current by properly adjusting the structure parameters of the QDIP.

This work was supported by the U.S. Army Research Office under Contract No. DAAD19-01-1-0673. The authors would like to thank Dr. Bill Clark of Army Research Office for his interest and support in this work.

- ¹J. Philips, P. Bhattacharya, S. W. Kennerly, D. W. Beekman, and M. Dutta, *IEEE J. Quantum Electron.* **35**, 936 (1999).
- ²S. Kim, H. Mohseni, M. Erdtmann, E. Michel, C. Jelen, and M. Razeghi, *Appl. Phys. Lett.* **73**, 963 (1998).
- ³S. J. Xu, S. J. Chua, T. Mei, X. C. Wang, X. H. Zhang, G. Karunasiri, W. J. Fan, C. H. Wang, J. Jiang, S. Wang, and X. G. Xie, *Appl. Phys. Lett.* **73**, 3153 (1998).
- ⁴D. Pan, E. Towe, and S. Kennerly, *Appl. Phys. Lett.* **75**, 2719 (1998).
- ⁵S. Y. Wang, S. D. Lin, H. W. Wu, and C. P. Lee, *Infrared Phys. Technol.* **42**, 473 (2001).
- ⁶Z. H. Chen, O. Baklenov, E. T. Kim, I. Mukhametzhanov, J. Tie, A. Madhukar, Z. Ye, and J. C. Campbell, *Infrared Phys. Technol.* **42**, 479 (2001).
- ⁷S. F. Tang, S. Y. Lin, and S. C. Lee, *Appl. Phys. Lett.* **78**, 2428 (2001).
- ⁸L. Jiang, S. S. Li, M. Z. Tidrow, W. R. Dyer, W. K. Liu, J. M. Fastenau, and T. R. Yurasits, *Appl. Phys. Lett.* **79**, 2982 (2001).
- ⁹V. Ryzhii, *Semicond. Sci. Technol.* **11**, 759 (1996).
- ¹⁰S. Maimon, E. Finkman, G. Bahir, S. E. Schacham, J. M. Garcia, and P. M. Petroff, *Appl. Phys. Lett.* **73**, 2003 (1998).
- ¹¹M. Grundmann, O. Stier, and D. Bimberg, *Phys. Rev. B* **52**, 969 (1995).
- ¹²H. Jiang and J. Singh, *Phys. Rev. B* **56**, 4696 (1997).
- ¹³X. Jiang, S. S. Li, and M. Z. Tidrow, *Physica E (Amsterdam)* **5**, 27 (1999).
- ¹⁴Adrienne D. Stiff, S. Krishna, P. Bhattacharya, and S. W. Kennerly, *IEEE J. Quantum Electron.* **37**, 936 (2001).
- ¹⁵B. F. Levine, *J. Appl. Phys.* **74**, R1 (1993).